Journal of Alloys and Compounds 619 (2015) 205–210

Contents lists available at ScienceDirect

Journal of Alloys and Compounds

journal homepage: www.elsevier.com/locate/jalcom

Pitting corrosion behavior in advanced high strength steels

Il-Jeong Park, Sang-Min Lee, Minwoo Kang, Sukjin Lee, Young-Kook Lee *

Department of Materials Science and Engineering, Yonsei University, 50 Yonsei-ro, Seoul, Republic of Korea

ARTICLE INFO

Article history:
Received 19 March 2014
Received in revised form 18 August 2014
Accepted 28 August 2014
Available online 16 September 2014

Keywords:
Advanced high strength steels
Pitting corrosion
Corrosion rate
Inclusions

ABSTRACT

The type and size of inclusions and their pitting corrosion behavior in dual-phase (DP), transformation-induced plasticity (TRIP), and twinning-induced plasticity (TWIP) steels were investigated. Whereas DP steel had single MnS inclusions, TRIP and TWIP steels had the complex inclusions of MnS and Al_2O_3, and MnS and Mn oxy-sulfide, respectively. TWIP steel had the most wide size distribution and the largest average size of inclusions. DP steel exhibited the lowest resistance to pitting corrosion due to the high density of inclusions. MnS inclusions in TRIP steel and Mn oxy-sulfide inclusions in TWIP steel acted as a galvanic anode in complex inclusions.

1. Introduction

Various stainless steels [1–6] and advanced high strength steels (AHSSs), such as dual-phase (DP) [7–11], transformation-induced plasticity (TRIP) [8–16], and twinning-induced plasticity (TWIP) [12,17–23] steels, have several different types of inclusions, which form during melting and casting [24]. Park et al. [25] observed single inclusions, such as MnS, AlN, Al_2O_3, and $MnAl_2O_4$, and complex inclusions in which two or more single inclusions were adjoined, such as MnS and AlN or MnS and Al_2O_3, in high Mn–Al steels. Gigacher et al. [26] reported that MnS grew on pre-existing $MnAl_2O_4$ spinel inclusions at temperatures ranging between liquidus and solidus temperatures in high Mn–Al steels. Complex inclusions consisting of MnS and Mn oxy-sulfide have been observed in duplex stainless steels [26,27].

Although these single and complex MnS inclusions improve materials machinability and reduce both tool wear and cutting force [28–30], they undermine hot ductility [32] and corrosion resistance [1–6,31–34] by providing pitting sites [1,2,34]. Park et al. [35] reported that DP steel with single MnS inclusions had the worse resistance to pitting corrosion than TRIP steel with single AlN inclusions. Grajcar et al. [36] reported that corrosion pits occurred intensively at single MnS inclusions in high Mn TWIP steels. However, the pitting corrosion behavior of complex inclusions including MnS in AHSSs has yet to be reported in detail unlike that of single MnS inclusions.

Therefore, the objective of the present study was to investigate pitting corrosion behavior, particularly at complex inclusions, in DP, TRIP, and TWIP steels through immersion and electrochemical polarization tests.

2. Experimental procedure

The commercial cold-rolled and annealed sheets of both DP and TRIP steels with a thickness of approximately 1.3 mm were used for the present study [35]. The Fe–18Mn–0.6C (wt.%) TWIP steel was melted using a vacuum-induction furnace and cast into a mold to make an ingot of 20 kgf. The ingot was reheated at 1150 °C for 1.5 h, hot-rolled at approximately 900 °C to a 2.5-mm thick plate, held at 450 °C for 1 h, and then air-cooled to room temperature. After surface descaling, the hot-rolled plate was cold-rolled to a thickness of 1.5 mm, annealed at 900 °C for 10 min, and then water-quenched to room temperature to prevent carbide precipitation. The chemical compositions of the three steels are listed in Table 1.

Annealed specimens were mechanically polished using sandpapers and diamond pastes, and then were etched by 4% nital and an aqueous solution of 100 g/L sodium metabisulfite ($Na_2S_2O_5$). The microstructures of the specimens were observed using an optical microscope (OM, Olympus, BX41M). The density and size of inclusions in each sample were statistically analyzed using OM images taken at a magnification of 1000. The types of inclusions were predicted using thermochemical computing software, FactSage 6.2 (ESM Software, Hamilton, OH) with the FSSTEL steel database.

The corrosion properties of each specimen were evaluated through immersion and electrochemical polarization tests in a neutral aqueous solution of 3.5 wt.% NaCl. Specimens for immersion tests measuring 15 mm wide and 15 mm long were polished using the paste with diamond particles of 1 μm, and ultrasonically cleaned in acetone, followed by weighing using a digit electronic balance with a precision of 1/10,000 before weight loss test. After completion of the tests, the corroded specimens were rinsed with distilled water. The corrosion products were removed using a smooth brush, then rinsed and dried again. The weight loss of each specimen during the 24-h immersion test was measured to calculate the corrosion rate, which was performed in a deaerated aqueous solution of 3.5 wt.% NaCl with constant stirring at various temperatures ranging from 2 °C to 100 °C. The corrosion rate (V_p) was calculated using the following equation [37]:

* Corresponding author. Tel.: +82 2 2123 2831.
E-mail address: yklee@yonsei.ac.kr (Y.-K. Lee).

http://dx.doi.org/10.1016/j.jallcom.2014.08.243
0925-8388/

Table 1
Chemical compositions of three steels used in the present study (in wt.%).

Steel	Mn	C	Al	Si	N	O	P	S	Fe
DP	2.07	0.06	–	0.04	0.004	0.002	0.011	0.010	Bal.
TRIP	1.52	0.20	1.08	0.28	0.009	0.002	0.008	0.006	Bal.
TWIP	17.65	0.62	–	0.04	0.012	0.004	0.012	0.006	Bal.

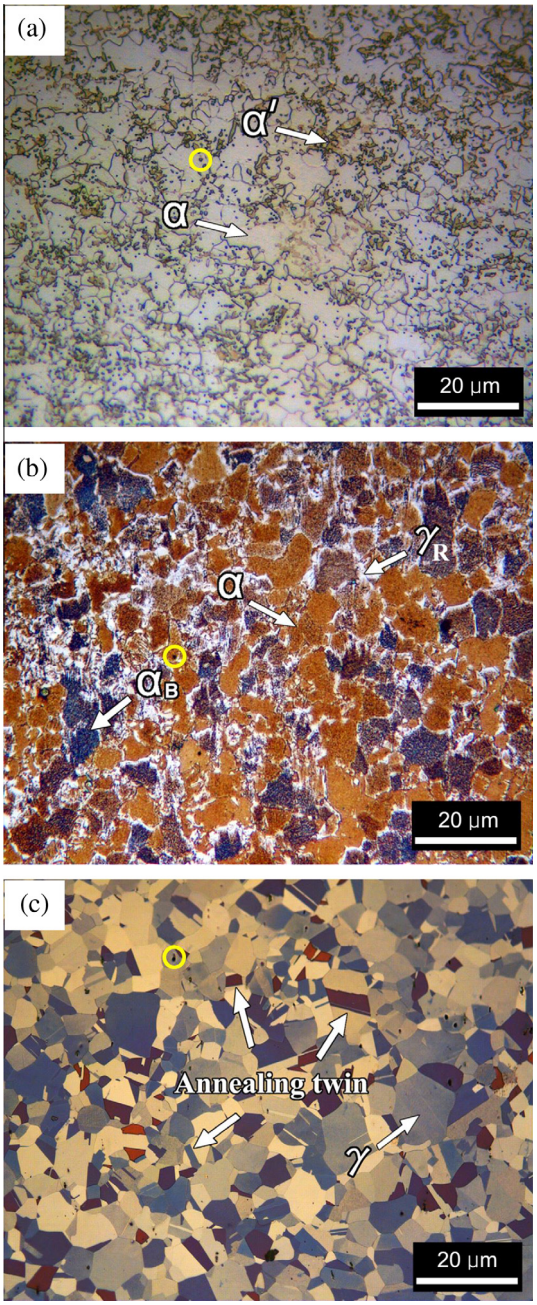

Fig. 1. Optical micrographs of (a) DP, (b) TRIP, and (c) TWIP steels annealed at 900 °C for 10 min after cold rolling. Yellow circles indicate inclusions. α is ferrite, α′ martensite, α_B bainite, γ_R retained austenite, and γ austenite. (For interpretation of the references to colour in this figure legend, the reader is referred to the web version of this article.)

$$R_{mass} = \frac{m_0 - m_1}{S_0 t} \quad (1)$$

$$V_p \text{ (mm per year)} = \frac{R_{mass}}{\rho} \times \frac{24 \times 365}{1000} = 8.76 \times \frac{R_{mass}}{\rho} \quad (2)$$

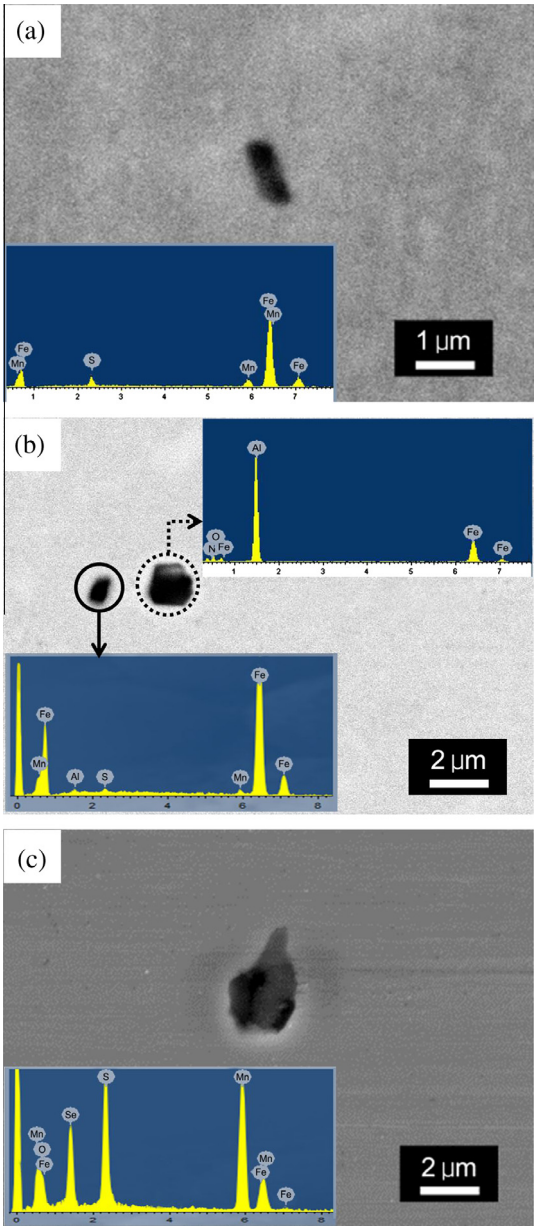

Fig. 2. SEM images showing (a) a MnS inclusion in DP steel, (b) MnS, AlN, and Al_2O_3 inclusions in TRIP steel, and (c) MnS and MnO inclusions in TWIP steel.

where m_0 and m_1 are the original weight and final weight of specimens, respectively (mg), S_0 is the exposed surface area of specimens (cm^2), t represents the immersion time (h), and ρ the steel density (7.86 g/cm^3).

To measure the corrosion current density (I_{corr}) of each specimen, electrochemical polarization tests were conducted in a deaerated aqueous solution of 3.5 wt.% NaCl without stirring at room temperature according to the ASTM G 5. Each specimen was coupled to a copper wire by soldering using the 95 Sn–5 Sb (wt.%) solder, and then mounted using epoxy resin. One side of mounted samples was ground to 600 grit using SiC abrasion papers. Except for the exposed area of each specimen (1 cm^2), the remainder was painted with transparent lacquer. Polarization tests were conducted at a potential range from −1.2 V_{SCE} to 0.2 V_{SCE} with a scanning rate of 1 mV/s using a potentiostat (EG&G, Model 263A). The counter electrode was a high-density graphite rod and the reference electrode was a saturated calomel electrode (SCE). The I_{corr} was commonly determined by the extrapolation of the cathodic and anodic curves between 50 and 100 mV away from the corrosion potential using corrosion analysis software (EG&G Princeton Applied Research, model 352/252, version 2.23) [38].

Inclusions and their initial pits were observed using a field-emission scanning-electron microscope (FE-SEM, JEOL, JSM7001F) attached with an energy dispersive X-ray spectroscope (EDXS, Oxford, INCA Energy).